NTU Journal of Engineering and Technology (2023) 2 (3) : 27-33
DOI: https://doi.org/10.56286/ntujet.v2i3.692

IRAQI Academic Scientific Journals

P-ISSN: 2788-9971 E-ISSN: 2788-998X
NTU Journal of Engineering and Technology
Available online at: https://journals.ntu.edu.iq/index.php/NTU-JET/index

A Robust U-Net-Based Approach for Accurate Brain Tumor Segmentation Using Multimodal MRI Data

Mohammed Talal Ghazal[1]
Technical Engineering College of Mosul, Northern Technical University, Iraq
mohammed.ghazal@ntu.edu.iq

Article Informations

Received: 13-09- 2023,
Revised : 18 -10-2023
Accepted: 20-10-2023,
Published online: 19-11-2023

Corresponding author:
Name: Mohammed T. Ghazal
Affiliation : Northern Technical University
Email:mohammed.ghazal@ntu.edu.iq

Key Words:
Brain Tumor,
Segmentation,
MRI,
U-Net,
BraTS-19.

A B S T R A C T

Detecting and quantifying the extent of brain tumors poses a formidable challenge in medical centers. Magnetic Resonance Imaging (MRI) has developed as a non-invasive brain cancers' primary diagnostic tool, offering the crucial advantage of avoiding ionizing radiation. Brain tumor manually segmented boundaries within 3D MRI volumes is an exceedingly time-intensive task, heavily reliant on operator expertise. Among brain tumors, gliomas stand out as the prevalent and highly malignant, significantly impacting patients' life expectancy, particularly at their highest grade. Recognizing the pressing need for a reliable, completely automatic segmentation technique to efficiently assess tumor extent, this study introduces a robust approach. A completely automated brain tumor segmentation method is proposed, leveraging U-Net-based deep convolutional networks. This approach underwent rigorous evaluation on the Multimodal Brain Tumor Image Segmentation BraTS-19 dataset a widely recognized medical image analysis dataset featuring multimodal MRI scans of brain tumors, including glioblastoma, anaplastic astrocytoma, and lower-grade glioma, coupled with corresponding manual tumor segmentations. This dataset serves as a pivotal resource for advancing automatic brain tumor segmentation techniques and assessing their performance using metrics like the Dice score, which achieved 92% for entire tumor. Cross-validation results affirm the efficiency and promise of our method in achieving accurate segmentation.

Introduction

Brain tumors, particularly primary malignant variants, represent a formidable challenge in the landscape of cancer [1,2]. Beyond their dismal prognoses, these tumors exert direct effects on cognitive performance and general quality of life [3,4]. Gliomas, which originate from brain glial cells, stand out as a predominant form of primary brain tumor in adults, loom large, accounting for nearly 80% of malignant cases [5,6]. Gliomas manifest as a diverse spectrum, encompassing slow-growing 'low-grade' tumors with relatively favorable prognoses and the more dangerous, highly infiltrative high-grade gliomas (HGG), such as glioblastoma, necessitating immediate intervention. Some malignant brain tumors persist although substantial improvements in imaging, radiation, chemotherapy, and surgical techniques, such as high-grade glioblastoma and metastases, remain recalcitrant, boasting a 2.5-year relative prognosis cumulatively rate of merely 8% and a stark 2% at the decade mark [7]. Moreover, outcomes for Those who have LGG (low-grade gliomas) exhibit notable variability, with an average survival rate of 10 years hovering around 57% [8]. Recent research has underscored the potential of magnetic resonance imaging (MRI) characteristics in the early diagnosis and treatment planning of brain tumors [9,10,11]. Multimodal MRI protocols, incorporating various imaging sequences, are routinely employed to assess critical factors such as Blood-brain barrier (BBB) integrity, cellularity, and vascularity of brain tumors. This strategic utilization of diverse image contrasts enhances the understanding of tumor biology. Typical MRI protocols for brain tumor evaluation commonly involve T1-weighted, T2-weighted (including Fluid-Attenuated Inversion Recovery, abbreviated as FLAIR), and gadolinium-enhanced T1-weighted imaging sequences. These structural MRI images play a substantial role in diagnosing most cases [12,13]. Image segmentation emerges as a pivotal step in extracting valuable insights from MRI images for brain tumor studies. It serves multiple critical purposes:

1. Precise delineation of the brain tumor extent: This effectively removes any confusing structures originating from other brain tissues, thus facilitating accurate sub-type classification and informed diagnosis.
2. Essential in radiotherapy or surgical planning: It ensures meticulous outlining of the brain tumor while excluding surrounding healthy tissues to avert inadvertent damage to language, motor, and sensory function sites during therapy.
3. Efficient monitoring of brain tumor recurrence: This is achieved through segmentation of longitudinal MRI scans.

Presently, clinical practice still heavily relies on manual segmentation performed by human operators. This labor-intensive manual process often involves slice-by-slice procedures, yielding results significantly influenced by operator experience and subjective judgment. Achieving reproducible results, even when performed by the same operator, remains a daunting challenge. In the context of multi-institutional, multimodal, and longitudinal clinical trials, there is a growing demand for Completely automated, unbiased, and consistent segmentation methods. In spite of recent advancements in both semi-automated and fully automated algorithms for brain tumor segmentation, numerous formidable challenges endure, chiefly stemming from the substantial variation observed among brain tumors in terms of size, shape, regularity, location, and their diverse appearances, including Contrasting uptake, image equality, and texture [11, 13]. Additionally, potential complexities in brain tumor segmentation arise from factors such as the intact BBB in LGG cases, leading to often invisible or indistinct tumor boundaries, and the irregular boundaries and discontinuities associated with aggressive tumor infiltration in high-grade gliomas (HGG) [14]. Furthermore, the visibility of various tumor subregions and types often necessitates the consideration of multimodal MRI data, posing challenges in co-registering sequences acquired at different spatial resolutions. Finally, the typical clinical MRI images' balance between in-plane and inter-slice resolution can impact segmentation accuracy due to Insufficient ratios of signal to noise SNR and the partial volume impact. Accurate segmentation of tumors within medical images holds paramount significance, offering critical insights essential for cancer analysis, diagnosis, treatment planning, and disease progression monitoring. In light of the challenges and complexities presented by brain tumors, this study endeavors to advance the Innovative in brain tumor segmentation, leveraging the power of deep learning and advanced imaging techniques. The objective is to develop a completely automated, objective, and reproducible segmentation method that addresses the intricacies of brain tumor diversity and aids clinicians in providing timely and accurate diagnoses, treatment planning, and patient management.

Literature Review

The preceding investigations into brain tumor segmentation can be broadly classified into the following categories:

Unsupervised Learning-Based Approaches: In earlier studies, researchers delved into unsupervised learning, focusing on clustering techniques to segment brain tumors. Hsieh et al. [15], for instance, combined fuzzy clustering and region-growing methods to delineate tumors based on T1-weighted

and T2-weighted sequences, yielding an accuracy of 73%. Another approach, featured in [16], introduced a multi-stage fuzzy c-means framework for multimodal MRI-based tumor segmentation, showcasing promising outcomes. However, it's worth noting that this framework was tested on a limited dataset. Recent work [17] assessed various clustering algorithms for glioblastoma segmentation, highlighting Gaussian hidden Markov random fields as superior to k-means, fuzzy k-means, and Gaussian mixture models. Yet, the best-performing algorithm in this study achieved an accuracy of only 77%.

Supervised Learning-Based Techniques: In contrast, supervised learning methods demand labeled training data to construct classification models for segmenting brain tumors. Wu et al. [18] applied super-pixel features within a conditional random fields framework, but the results exhibited significant variation among different patient cases, particularly underperforming in low-grade glioma (LGG) images. An alternative approach, presented in [19], harnessed extremely randomized forests to classify appearance and context-based features, achieving an 83% Dice score. More recently, a study [20] combined extremely randomized trees classification for a single FLAIR sequence-based image using super-pixel-based oversegmentation MRI scans, resulting in an impressive 88% overall Dice score for complete tumor segmentation in both LGG and high-grade glioma (HGG) cases. However, tuning super-pixel size and compactness remained a challenge.

Deep Learning-Based Innovations: Recent strides in deep learning have propelled brain tumor segmentation, relying on convolutional neural networks (CNNs) to automatically learn intricate features directly from data. These deep CNNs have demonstrated remarkable success in the Brain Tumor Image Segmentation (BRATS) competition, consistently ranking at the top [21,22]. The power of deep CNNs arises from their layered architecture, involving multiple convolutional layers that learn progressively complex features. Nonetheless, several challenges persist, including the inherently abnormal nature of tumor segmentation, the ongoing difficulty in accurately segmenting low-grade gliomas, limitations in delineating core and infiltrative tumor regions, and the demand for more computationally efficient methods.

Clustering Methods and Unsupervised Learning: Early endeavors in brain tumor segmentation explored unsupervised learning approaches, where researchers aimed to cluster similar data points to segment tumors. Notably, Hsieh et al. (2014) fused fuzzy clustering with region-growing techniques to achieve a 73% segmentation accuracy based on T1-weighted and T2-weighted sequences. A multi-stage fuzzy c-means framework was introduced in [16] to segment brain tumors from multimodal MRI, showing promise despite its evaluation on a limited dataset. Additionally, [17] undertook an evaluation of various clustering algorithms for glioblastoma segmentation, highlighting the superiority of Gaussian hidden Markov random fields.

Supervised Learning and Classification Models: Supervised learning-based methods emerged as a prominent avenue, necessitating labeled training data for constructing classification models. Wu et al. (2015) harnessed super-pixel features within a conditional random field's framework for brain tumor segmentation, with performance variations observed among different patient cases. Extremely randomized forests were employed in [19] to classify appearance and context-based features, achieving an 83% Dice score. A recent study [20] combined this classification approach with super-pixel-based over-segmentation for FLAIR sequence-based MRI scans, resulting in an impressive 88% Dice score for complete tumor segmentation.

Deep Learning Revolution: The advent of deep learning marked a transformative shift in brain tumor segmentation. Deep convolutional neural networks (CNNs) have taken center stage, automatically learning complex features directly from data. These deep CNNs have consistently dominated the Brain Tumor Image Segmentation (BRATS) competition [21,22]. The strength of deep CNNs lies in their multi-layered architecture, leveraging convolutional layers to capture progressively intricate features [23,24]. Nevertheless, several challenges persist, including the unique nature of tumor segmentation, the ongoing difficulty in segmenting low-grade gliomas, limitations in delineating core and infiltrative tumor regions, and the imperative need for more computationally efficient methods.

Methodology

The research hinged on the 2019 Brain Tumour Segmentation Challenge (BraTS) dataset, a cornerstone in advancing the field of brain tumor segmentation [25,26]. This dataset was thoughtfully partitioned into a training set, where the proposed models underwent intensive training, and a validation set, meticulously crafted to serve as the benchmark for evaluating the ensemble approach [27,28]. Within the training set, we had a comprehensive cohort comprising 259 patients diagnosed with high-grade gliomas, alongside an additional 76 patients afflicted by low-grade gliomas. These data points served as the backbone for the proposed model training and were adorned with painstakingly crafted annotations provided by domain experts, ensuring the reliability of the ground truth labels. The validation set, distinctively, encompassed 125 cases, bearing an air of mystery as the grades of these tumors were deliberately kept

undisclosed from the public [29,30]. This multi-institutional dataset was a result of collaborative efforts from 19 different contributors, making it a testament to the collaborative spirit in medical research. It boasted a rich variety of multimodal MRI scans for each patient, including essential sequences like T1, T1 contrast-enhanced (T1ce), T2-weighted (T2), and Fluid Attenuated Inversion Recovery (FLAIR). These sequences, each with its unique information, played a crucial role in the segmentation of various tumoral subregions. To ensure the quality and consistency of the dataset, this paper embarked on an extensive preprocessing journey. This involved the meticulous removal of extraneous elements through a process known as skull-stripping. Subsequently, researcher has been implemented alignment procedures to ensure the scans conformed precisely to a standardized anatomical template. The scans were further subjected to resampling, rendering them at a uniform resolution of $1mm^3$. Each sequence had volumetric dimensions of 240 × 240 × 155, providing an extensive view of the brain's internal structures. In Figure 1, we present a visually informative snapshot from the training set. It's essential to emphasize that the research methodology adhered rigorously to the exclusive use of the BraTS-19 dataset, underscoring the commitment to maintaining data integrity and avoiding external data sources. Furthermore, it's pertinent to note that the BraTS-19 test set was accessible only to registered challenge participants, leading us to report the test results solely on the BraTS-19 validation set. The analysis embarked on a comprehensive exploration, commencing with an in-depth examination of the segmentation results accomplished by the proposed network on this validation set. Subsequently, we ventured into a meticulous comparative assessment, pitting the results against established state-of-the-art architectures to validate the innovation and efficacy of the proposed approach.

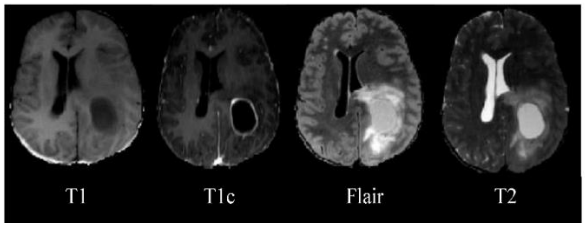

Figure 1. Example of the BraTS-19 Training Dataset. From left to right, show the axial slice of MRI images in Flair, T1, T1ce and T2.

Data augmentation is a strategic tool we employed with precision in this study, driven by the overarching goal of enhancing the network's performance. This technique operates by ingeniously generating a diverse array of training data from the original dataset, strategically enriching the learning process. The approach to data augmentation was a comprehensive one, incorporating an array of sophisticated methods to infuse versatility into the training data. These methods included fundamental operations like flipping, rotation, shift, and zoom. While these operations did introduce displacement fields within the images, it's crucial to note that they were meticulously calibrated to preserve the fundamental shapes and structures inherent to the brain tumor images. In essence, the data augmentation strategy was a meticulously orchestrated symphony, fine-tuned to bolster our network's capacity to generalize and learn from a more expansive and diverse dataset, all while respecting the inherent shapes and characteristics of the original images.

The proposed network architecture, inspired by the U-Net model which is shown in Figure 2, has been substantially enhanced to bolster its capacity to capture intricate features vital for precise segmentation. It comprises an extended down-sampling (encoding) path and a more robust up-sampling (decoding) path. In the down-sampling path, we've expanded the network to include a total of seven convolutional blocks, each housing a pair of convolutional layers. These layers utilize 3×3 filters, maintain a stride of 1 in both directions, and employ rectifier activation functions. This expansion significantly augments the number of feature maps, increasing it to an impressive 2048. To facilitate the down-sampling process, we've integrated max-pooling with a 2×2 stride at the end of each block, with the exception of the final one. This orchestrated progression effectively reduces the size of feature maps from an initial 240×240 down to a more compact 15×15. Conversely, in the up-sampling path, each block commences with a deconvolutional layer featuring 3×3 filters and a 2×2 stride. This operation efficiently doubles the size of feature maps in both dimensions while halving the amount of feature maps. Consequently, the feature maps expand in size from 15×15 to a comprehensive 240×240. Within each up-sampling block, two convolutional layers work cohesively to decrease the number of feature maps in the combination of deconvolutional feature maps and those originating from the encoding path. Moreover, we have adjusted various critical parameters. Zero-padding is strategically employed to ensure consistent output dimensions across all the CNN layers in both the down-sampling and thw up-sampling tracks. Additionally, the final segmentation output is derived through a 1×1 convolutional layer, efficiently reducing the amount of feature maps to two, signifying the foreground and background segmentation. It's worth highlighting that the network avoids the use of fully connected layers, opting for a more streamlined architecture that prioritizes efficiency and accuracy in the context of brain tumor segmentation. These enhancements empower the proposed model to capture intricate

details, making it an invaluable tool in the realm of medical image analysis. During the training phase, we employed a cross-entropy-based cost function, a fundamental choice for training deep neural networks. To optimize this cost function regarding the model's parameters, we harnessed the power of the Adaptive Moment Estimation (Adam) optimizer. Adam is a widely used optimization technique that leverages both the first and second moments of gradients to iteratively update and fine-tune the model's parameters. The specific configuration for the Adam optimizer involved setting a learning rate of 0.00001 and a maximum of 150 training epochs. To initiate the network, we initialized all weights from a normal distribution with a mean of 0 and a standard deviation of 0.01, while biases were initialized to 0.

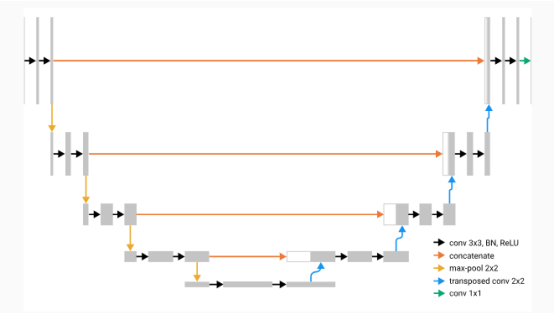

Figure 2. The architecture of U-Net model.

Experimental Work and Result

To evaluate the performance of the suggested U-Net model, we conducted extensive tests using the BraTS-19 dataset. Additionally, we performed a sequence of module validation experiments was conducted to confirm the effectiveness of each module introduced in this paper. We divided the BraTS-19 dataset into a training data (80%) and a testing data (20%), resulting in 268 training cases and 67 cases for testing. Beyond the Dice coefficient, additionally, we considered three additional essential evaluation metrics: Sensitivity, Specificity, and Hausdorff distance (Hausdor_95), as mandated by the competition which defined in the below equations. The model's performance, which is shown in Table 1, achieving Dice scores of 0.920, 0.90, and 0.865 on the entire tumor, central tumor, and enhanced tumor, respectively.
In the assessment, we employ a set of metrics to evaluate the model's performance. These metrics assist in assessing the accuracy of the predictions and their alignment with the ground truth:

True Positive (TP): This represents the count of correctly identified positive pixels.

False Positive (FP): It signifies the count of erroneously identified positive pixels.

- True Negative (TN): This measures the count of correctly identified negative pixels.
- False Negative (FN): It denotes the count of mistakenly identified negative pixels.

$$Dice = \frac{2TP}{FP + 2TP + FN} \quad \dots (1)$$

$$Sensitivity = \frac{TP}{TP + FN} \quad \dots (2)$$

$$Specificity = \frac{TN}{TN + FP} \quad \dots (3)$$

$$Haus(T,P) = \max\{\sup t \in T \inf p \in Pd(t,p), \sup p \in P\ inf\ t \in Td\ (t,p)\} \quad \dots (4)$$

We utilize 't' to represent the pixels within the ground-truth regions and 'p' for those within the predicted regions. The function 'd(t, p)' computes the distance between these pixels. The evaluation metrics encompass:

- Dice Coefficient: This metric evaluates the overall voxel-wise overlap between the predicted and ground-truth regions.
- Sensitivity: It assesses the model's capacity to accurately identify positive regions.
- Specificity: This metric gauges the model's ability to correctly exclude negative regions.
- Hausdorff Distance: It quantifies the maximum boundary separation between the predicted and ground-truth segmented regions.
- Hausdorff95: This metric provides insights into the 95% quantile of the surface distance distribution.

Table 1: The model's performance

Metric \ Type	Entire Tumor	Central Tumor	Enhanced Tumor
Dice	0.920	0.90	0.865
Sensitivity	0.892	0.881	0.865
Specificity	0.995	0.993	0.991
Hausdor_95	5.431	7.334	5.210

In Figure 3, each image comprises six columns, representing an axial MRI slice acquired in Flair, T1, T1ce, and T2 modalities, which serve as inputs for the proposed model. Additionally, it displays the ground truth (GT) and the model's prediction labels. Notably, the proposed model's segmentation results exhibit a remarkable resemblance to the Ground Truth. The model adeptly labels pixels in regions marked as enhancing, demonstrating precise identification. Moreover, the model effectively discerns pixels in areas without enhancing labels, contributing to a notable reduction in False Positives

(FP). These results substantiate the robustness and efficacy of the proposed U-Net model in the task of brain tumor segmentation, showcasing its potential for enhancing medical image analysis.

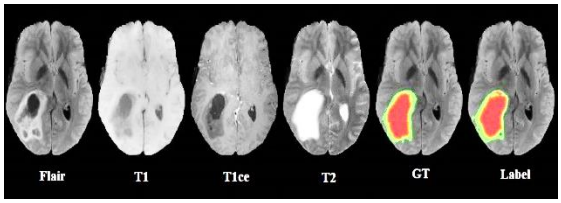

Figure 3. Example of segmentation results on the BraTS-19 Dataset.

Conclusion

This paper introduces a robust brain tumor segmentation approach based on the U-Net architecture. Using the BraTS-19 dataset, extensive experiments were conducted to validate each proposed module. The U-Net model achieved remarkable performance, with high scores in various metrics. Visual inspections confirmed its accuracy. A comprehensive set of evaluation metrics was employed, with the Dice coefficient being a primary metric. This work offers an advanced solution for brain tumor segmentation with potential clinical applications. The use of U-Net architecture, rigorous evaluation, and extensive experiments establishes the approach's effectiveness, promising improved medical applications.

References

[1] Liu, Zhihua, et al. "Deep learning based brain tumor segmentation: a survey." *Complex & intelligent systems* 9.1 (2023): 1001-1026.

[2] Raza, Rehan, et al. "dResU-Net: 3D deep residual U-Net based brain tumor segmentation from multimodal MRI." *Biomedical Signal Processing and Control* 79 (2023): 103861.

[3] Ramesh, Karthik K., et al. "A Fully Automated Post-Surgical Brain Tumor Segmentation Model for Radiation Treatment Planning and Longitudinal Tracking." *Cancers* 15.15 (2023): 3956.

[4] Balaha, Hossam Magdy, and Asmaa El-Sayed Hassan. "A variate brain tumor segmentation, optimization, and recognition framework." *Artificial Intelligence Review* 56.7 (2023): 7403-7456.

[5] Cao, Yuan, et al. "MBANet: A 3D convolutional neural network with multi-branch attention for brain tumor segmentation from MRI images." Biomedical Signal Processing and Control 80 (2023): 104296.

[6] Schwartzbaum, J.A., Fisher, J.L., Aldape, K.D., Wrensch, M.: Epidemiology and molecular pathology of glioma. Nat. Clin. Pract. Neurol. 2, 494–503 (2006).

[7] Smoll, N.R., Schaller, K., Gautschi, O.P.: Long-term survival of patients with glioblastoma multiforme (GBM). J. Clin. Neurosci. 20, 670–675 (2013).

[8] Ramakrishna, R., Hebb, A., Barber, J., Rostomily, R., Silbergeld, D.:Outcomes in Reoperated Low-Grade Gliomas. Neurosurgery. 77, 175–184 (2015).

[9] Mazzara, G.P., Velthuizen, R.P., Pearlman, J.L., Greenberg, H.M., Wagner, H.: Brain tumor target volume determination for radiation treatment planning through automated MRI segmentation. Int. J. Radiat. Oncol. Biol. Phys. 59,300–12 (2004).

[10] Yamahara, T., Numa, Y., Oishi, T., Kawaguchi, T., Seno, T., Asai, A., Kawamoto, K.: Morphological and flow cytometric analysis of cell infiltration in glioblastoma: a comparison of autopsy brain and neuroimaging. Brain Tumor Pathol. 27, 81–7 (2010).

[11] Bauer, S., Wiest, R., Nolte, L.-P., Reyes, M.: A survey of MRI-based medical image analysis for brain tumor studies. Phys. Med. Biol. 58, R97-129 (2013).

[12] Jones, T.L., Byrnes, T.J., Yang, G., Howe, F. a, Bell, B.A., Barrick, T.R.: Brain tumor classification using the diffusion tensor image segmentation (DSEG) technique. Neuro. Oncol. 17, 466–476 (2014).

[13] S. Bauer, R. Wiest, L. P. Nolte, and M. Reyes. (2013). A Survey of MRI-Based Medical Image Analysis for Brain Tumour Studies. [Online].

[14] R. Leece, J. Xu, Q. T. Ostrom, Y. Chen, C. Kruchko, and J. S. Barnholtz-Sloan, ``Global incidence of malignant brain and other central nervous system tumors by histology, 2003_2007," NeuroOncology, vol. 19, no. 11, pp. 1553_1564, Oct. 2017.

[15] Hsieh, T.M., Liu, Y.-M., Liao, C.-C., Xiao, F., Chiang, I.-J., Wong, J.-M.: Automatic segmentation of meningioma from non-contrasted brain MRI integrating fuzzy clustering and region growing. BMC Med. Inform. Decis. Mak. 11, 54 (2011).

[16] Szilágyi, L., Lefkovits, L., Benyó, B.: Automatic Brain Tumor Segmentation in multispectral MRI volumes using a fuzzy c-means cascade algorithm. In: 2015 12th International Conference on Fuzzy Systems and Knowledge Discovery (FSKD). pp. 285–291 (2015).

[17] Juan-Albarracín, J., Fuster-Garcia, E., Manjón, J. V, Robles, M., Aparici, F., Martí-Bonmatí, L., García-Gómez, J.M.: Automated glioblastoma segmentation based on a multiparametric structured unsupervised classification. PLoS One. 10, e0125143 (2015).

[18] Wu, W., Chen, A.Y.C., Zhao, L., Corso, J.J.: Brain tumor detection and segmentation in a CRF (conditional random fields) framework with pixelpairwise affinity and superpixel-level features. Int. J. Comput. Assist. Radiol. Surg. (2013).

[19] Pinto, A., Pereira, S., Correia, H., Oliveira, J., Rasteiro, D.M.L.D., Silva, C.A.: Brain Tumour Segmentation based on Extremely Randomized

Forest with high-level features. In: 2015 37th Annual International Conference of the IEEE Engineering in Medicine and Biology Society (EMBC). pp. 3037–3040 (2015).

[20] Soltaninejad, M., Yang, G., Lambrou, T., Allinson, N., Jones, T.L., Barrick, T.R., Howe, F.A., Ye, X.: Automated brain tumour detection and segmentation using superpixel-based extremely randomized trees in FLAIR MRI. Int. J. Comput. Assist. Radiol. Surg. (2016).

[21] Pereira, S., Pinto, A., Alves, V., Silva, C.A.: Brain Tumor Segmentation using Convolutional Neural Networks in MRI Images. IEEE Trans. Med. Imaging. 35, 1240–1251 (2016).

[22] Kamnitsas, K., Ledig, C., Newcombe, V.F.J., Simpson, J.P., Kane, A.D., Menon, D.K., Rueckert, D., Glocker, B.: Efficient multi-scale 3D CNN with fully connected CRF for accurate brain lesion segmentation. Med. Image Anal. 36, 61–78 (2017).

[23] Ronneberger, O., Fischer, P., Brox, T.: U-Net: Convolutional Networks for Biomedical Image Segmentation. In: Medical Image Computing and Computer-Assisted Intervention. pp. 234–241 (2015).

[24] Milletari, F., Navab, N., Ahmadi, S.-A.: V-Net: Fully Convolutional Neural Networks for Volumetric Medical Image Segmentation. arXiv. 1–11 (2016).

[25] Cui S, Mao L, Jiang J, Liu C, Xiong S (2018). Automatic semantic segmentation of brain gliomas from MRI images using a deep cascaded neural network. J Healthcare Engineering, 2018, 1-14.

[26] Khawaldeh S, Pervaiz U, Rafiq A, Rami SA (2017). Noninvasive grading of glioma tumor using magnetic resonance imaging with convolutional neural networks. Appl Sci, 8, 1-17.

[27] Chinmayi P, Agilandeeswari L, Prabu Kumar M, Muralibabu K (2017). An efficient deep learning neural network based brain tumor detection system. Int Pure Appl Mathemat, 117, 151-60.

[28] Konstantinos KK, Ledig C, Virginia, FJ, et al (2017). Efficient multi scale 3D CNN with fully connected CRF for accurate brain lesion segmentation. Med Image Analysis, 36, 61-78.

[29] S. Bakas et al., ``Identifying the best machine learning algorithms for brain tumor segmentation, progression assessment, and overall survival prediction in the BRATS challenge," 2018, arXiv:1811.02629. [Online]. Available: https://arxiv.org/abs/1811.02629

[30] S. Bakas, H. Akbari, A. Sotiras, M. Bilello, M. Rozycki, J. S. Kirby, J. B. Freymann, K. Farahani, and C. Davatzikos, ``Advancing the cancer genome atlas glioma MRI collections with expert segmentation labels and radiomic features," Sci. Data, vol. 4, no. 1, Dec. 2017, Art. no. 170117.